AIAA 80-0281R

Determination of Solid Propellant Admittances by the Impedance Tube Method

J. D. Baum,* B. R. Daniel,† and B. T. Zinn‡
Georgia Institute of Technology, Atlanta, Ga.

The adaptation of the impedance tube technique for the measurement of solid propellant admittances and response functions is described. These quantities are needed for combustion stability analysis of solid rocket motors. The experimental set up consists of a tube with a disk of solid propellant sample placed at one end and a combination of an exhaust valve and an acoustic driver placed at the other end. Performing a test consists of turning on the acoustic driver to excite a standing wave of a predetermined frequency in the tube, ignition, and burnout of the solid propellant sample. During a test, acoustic pressure data is measured by fifteen pressure transducers distributed along a distance that includes, at least, two standing wave pressure minima. The data are transferred via a fast analog-to-digital convertor to a minicomputer system for immediate storage and later analysis. The measured acoustic pressure amplitude and phase data are input into a newly developed data reduction procedure that is based upon the solution of the impedance tube wave equations, for the determination of the admittance and response function of the tested solid propellant sample and the acoustic energy losses in the gas phase. The paper presents results obtained in a series of tests conducted with an A-14 propellant. The paper demonstrates the capability of the developed experimental technique to determine simultaneously the acoustic characteristics of the flow inside the impedance tube and the admittance of the burning solid propellant for the duration of the experiment.

Nomenclature

A_{ij} = defined in the Appendix
C = constant defined in Eq. (8)
$\bar{c}$ = velocity of sound, m/s
c_p = specific heat at constant pressure, kcal/kg K
c_v = specific heat at constant volume, kcal/kg K
E = error function defined in Eq. (15), $(N/m^2)^2$ or Pa^2
F = losses due to viscosity and gas phase damping, $kg/m^2\ s^2$
G = gas phase bulk loss coefficient, $kg/m^3\ s$
I = identity matrix
M = Mach number
m = mass flow rate per unit cross-sectional area, $kg/m^2\ s$
p = pressure, N/m^2 or Pa
Q = volumetric heat source, $kcal/m^3\ s$ mole
R = gas constant, kcal/kg mole K
r = burning rate, m/s
s = entropy, kcal/kg K
T = temperature, K; also transmission matrix defined in Eq. (10)
T_{w0} = wall temperature at $x=0$, K
u = axial velocity, m/s
Y = specific admittance, dimensionless
Z = variable used to represent oscillatory quantities, defined by Eq. (6)
ρ_s = density of solid propellant, kg/m^3
ρ = density, kg/m^3

Superscripts

$\bar{()}$ = variable describing a steady-state quantity
$()'$ = variable describing a perturbation quantity

Subscripts

b = quantity evaluated at the propellant surface
w = quantity evaluated at the wall
R = real part of a complex quantity
I = imaginary part of a complex quantity

Presented as Paper 80-0281 at the AIAA 18th Aerospace Sciences Meeting, Pasadena, Calif., Jan. 14-16, 1980; submitted Feb. 6, 1980; revision received July 15, 1980.

*Graduate Research Assistant, School of Aerospace Engineering.
†Senior Research Engineer, School of Aerospace Engineering.
‡Regents' Professor, School of Aerospace Engineering. Associate Fellow AIAA.

Introduction

RECENT advances made in the application of the modified impedance tube technique in the measurement of solid propellant admittances and response functions are described. The solid propellant admittance, defined as the complex ratio of the velocity perturbation normal to the propellant surface and the pressure perturbation evaluated at the propellant surface, is a measure of the amplification (or attenuation) sustained by a gas phase disturbance upon interaction with the combustion process at the solid propellant surface. Consequently, the admittances of solid propellants are used to evaluate the relative driving characteristics of various solid propellants. In addition, since the stability of a solid rocket depends upon the energy balance between various processes that contribute to the combustor disturbance attenuation or amplification, the ability to determine quantitatively the admittance of the burning solid propellant is of utmost importance for the development of a capability for designing stable rocket motors. The development of an experimental technique capable of measuring the admittances and response functions of burning solid propellants under conditions simulating those experienced by unstable solid rockets is the main objective of the research work described in this paper.

To date, most response function measurements were performed utilizing the self-excited T-burner technique.[1] When weakly driving and aluminized propellants failed to generate the desired oscillations in the T-burner, the variable area T-burner[2] and the pulsed T-burner[3] were developed. However, due to difficulties associated with the interpretation of T-burner data, additional experimental techniques such as the rotating valve,[4] microwave,[5] and the impedance tube[6,7] have recently been developed for the measurement of burning solid propellant response functions. Comparisons of the data

generated by these various experimental techniques would hopefully result in accurate solid propellant response function data.

A schematic of the modified impedance tube is shown in Fig. 1. The tested solid propellant disk is placed at one end of the tube and a combination of an acoustic driver and an exhaust valve is placed at the opposite end. Performing a test consists of turning on the acoustic driver to excite a standing wave of a predetermined frequency in the tube and the ignition and burn out of the tested solid propellant sample. During the test, heat losses to the tube walls and the presence of waves moving in both directions result in an axially varying steady temperature profile and a standing acoustic wave in the tube. It can be shown that the characteristics of the resulting standing wave are dependent, among other things, upon the boundary conditions at the burning propellant surface that can be described under isentropic conditions by specifying the propellant surface admittance. It can also be shown[8] that the magnitude and sign of the real part of the admittance are related directly to the magnitude and direction of acoustic energy flow at the burning propellant surface. When the real part of the admittance is positive, acoustic energy is flowing from the combustion zone into the impedance tube and the propellant is said to be driving. When this occurs, disturbances in the gas phase are amplified by the combustion process at the propellant surface.

In the impedance tube experiment, the relationship between the admittance at the burning solid propellant surface and the impedance tube wave structure is utilized to determine the admittance at the propellant surface. This is accomplished by measuring the resulting acoustic wave structure and relating it to the unknown admittance by utilizing the solutions of the impedance tube wave equations.

During a test, fifteen pressure transducers are placed at predetermined locations along the tube walls to measure the acoustic pressure amplitudes and phases. The data acquired at different instances during the test period are input into a newly developed data reduction scheme that determines the admittance and response function at the burning solid propellant surface. This paper describes recent efforts that were concerned with improvement of the data acquisition system and the development of a new data reduction scheme. In addition, results obtained in tests conducted with a composite solid propellant (i.e., A-14) are presented and discussed.

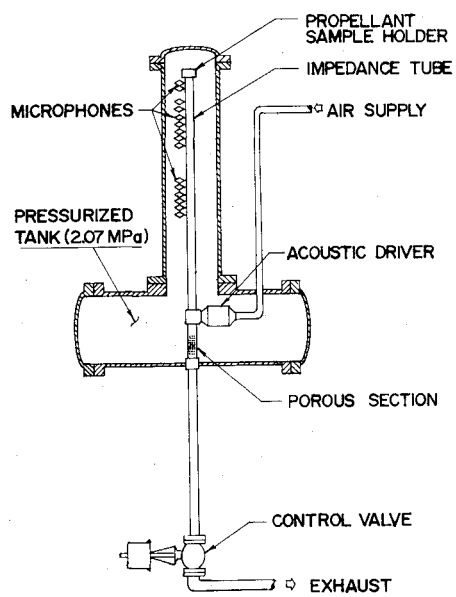

Fig. 1 Schematic diagram of pressurized impedance tube facility.

Improved Data Reduction Procedure

A new data reduction procedure that utilizes acoustic pressure amplitude and phase data measured at discrete points along the wall of the impedance tube for the determination of the admittance of the tested solid propellant, is outlined in this section. To develop the needed data reduction scheme, the assumptions introduced in Ref. 7 for describing the impedance tube flow are utilized. Under these assumptions, the flow inside the tube can be described by the following set of one-dimensional conservation equations:

Continuity

$$\frac{\partial \rho}{\partial t} + \frac{\partial}{\partial x}(\rho u) = 0 \tag{1}$$

Momentum

$$\frac{\partial}{\partial t}(\rho u) + \frac{\partial}{\partial x}(\rho u^2) = \frac{-\partial p}{\partial x} - F \tag{2}$$

Energy

$$\rho T\left(\frac{\partial s}{\partial t} + u\frac{\partial s}{\partial x}\right) = c_v \frac{Q}{R} \tag{3}$$

State

$$p = \rho R T \tag{4}$$

First and second laws of thermodynamics

$$\mathrm{d}s = c_p \frac{\mathrm{d}T}{T} - R\frac{\mathrm{d}p}{p} \tag{5}$$

Next, each of the following dependent variables is expressed as a sum of a steady-state solution and a time-dependent perturbation [e.g., $p(x,t) = \bar{p}(x) + p'(x,t)$] and these expressions are substituted into Eqs. (1-5). Separating the resulting equations into the corresponding steady state and unsteady systems of equations, linearizing the unsteady equations assuming that the solutions are periodic in time [i.e., $p'(x,t)\alpha e^{i\omega t}$], as is the case in the impedance tube experiment, using the relation $F' = Gu'$ (where G is a constant) yields a system of linear wave equations that can be expressed in the following form

$$\frac{\mathrm{d}Z_i}{\mathrm{d}x} = \sum_{j=1}^{3} A_{ij} Z_j \qquad i = 1,2,3 \tag{6}$$

Where Z_1, Z_2, and Z_3, respectively, represent u', p' and ρ'. The coefficients A_{ij} depend upon the corresponding steady-state solutions and the acoustic energy gas phase loss that is specified by a parameter G. Expressions for the coefficients A_{ij} are given in the Appendix.

Before proceeding with the solution of Eq. (6), a comment regarding the determination of the steady-state solution is in order. Analysis of the corresponding steady-state conservation equations shows that once the behavior of one of the dependent variables is known, the remaining dependent variables could be determined by utilizing the steady-state conservation equations. Experiments and related analytical studies[7] conducted earlier under this investigation had shown that a steady-state temperature distribution that is consistent with the one-dimensional description of the wave propagation problem in the impedance tube is provided by the following expression:

$$T(x) = T_w(x) + [T_c - T_{w_0}]e^{-x/\Lambda} \tag{7}$$

where

$$\Lambda = C\{1 + [T_w(x)/\bar{T}(x)]\}^n; \quad n = 0.68 \tag{8}$$

Examination of the above equation shows that $\bar{T}(x)$ can be determined once the constants T_c, C, and the wall temperature distribution $T_w(x)$ are known. It is of interest to note that since C controls the axial temperature variation along the tube, it also influences the tube's acoustic wave structure through its influence upon the sound speed variation. In the present study the as yet unknown constant C is determined from the measured acoustic pressure data, as is described subsequently.

Proceeding with the description of the data reduction procedure, Eq. (6) is rewritten in the following form

$$\{Z'\}_x = [A]_x \{Z\}_x \tag{9}$$

where the subscript x represents the location at which the elements of the matrix are evaluated and the superscript denotes differentiation with respect to x. To evaluate the coefficients A_{ij}, the values of the gas phase loss coefficient G and the constant C [i.e., see Eq. (8)] must be known. Equation (9) consists of a system of three linear, homogeneous coupled first-order ordinary differential equations that can be treated as an initial value problem once the dependent variables u', p' and ρ' are known at $x=0$ location and the coefficient matrix $[A]_x$ is known throughout the domain of interest of x. While in principle p', ρ', and u' could be measured at some location, the accurate measurement of u' and ρ' is extremely difficult in practice. To circumvent this difficulty, the "transmission matrix" T (Ref. 9) has been introduced in order to relate the measured acoustic pressure data to the needed initial value data (i.e., u' and ρ' at the initial point $x=0$). Utilizing the transmission matrix T, one can write

$$\{Z\}_x = [T]_x \{Z\}_{x_0} \tag{10}$$

where $\{Z\}_{x_0}$ represents values of the dependent variables at the initial location x_0. Equation (10) can be rewritten as

$$\{Z\}_{x_0} = [T]_x^{-1} \{Z\}_x \tag{11}$$

Next, differentiating Eq. (10) with respect to x, solving the resultant equation for $\{Z\}_{x_0}$ and substituting the results into Eq. (11) yields

$$\{Z'\}_x = [T']_x [T]_x^{-1} \{Z\}_x \tag{12}$$

Finally, a comparison of Eqs. (12) and (9) gives

$$[T']_x = [A]_x [T]_x \tag{13}$$

where

$$[T]_{x=0} = I \tag{14}$$

Thus, once $[A]_x$ is known, the matrix $[T]_x$ can be determined by forward integration of Eq. (13), beginning at $x=0$. By utilizing Eq. (10) and the computed $[T]_x$ matrix, $\{Z\}_x$ can be determined once $\{Z\}_{x_0}$ is known.

To determine the unknown $\{Z\}_{x_0}$, the following error function E is introduced:

$$E = \sum_{i=1}^{n} \left[(p'_{e_i} - p'_{t_i}) \left(\frac{p'_{e_1}}{p'_{e_i}} \right) \right]^2 \tag{15}$$

where p'_{e_i} is the measured (i.e., amplitude and phase which can be used to express p' as a complex number) acoustic pressure at location i and p_{t_i} is the corresponding, theoretically calculated complex acoustic pressure at location i.

The error function defined by Eq. (15) differs from the error function utilized earlier in this program (i.e., see Ref. 10) by the inclusion of the factor p'_{e_1}/p'_{e_i} where p'_{e_1} is measured near a pressure maxima, in the present definition. This is included in order to assure that all of the measured data contribute equally to the determination of the unknowns of the problem (i.e., $\{Z\}_{x_0}$, G, and C). In contrast, when the factor p'_{e_1}/p'_{e_i} is not included in the definition of E, acoustic pressure data measured near the standing wave maxima exerts considerably more influence upon the solution then pressure data measured near minima points of the standing wave.

The theoretical pressure p'_{t_i} and consequently the error function E are functions of the three as yet unknowns, initial conditions u', p', and ρ' at $x=0$, and the parameters G and C. The objective of the analysis is to find the values of these unknowns that minimize the error function E. Since the gradient of E has to vanish at the minimum, it follows that at the minimum E has to satisfy the following conditions:

$$\frac{\partial E}{\partial (Z_1)_{x_0}} = \frac{\partial E}{\partial (Z_2)_{x_0}} = \frac{\partial E}{\partial (Z_3)_{x_0}} = 0 \tag{16}$$

which can be rewritten, utilizing Eq. (15), as

$$\frac{\partial E}{\partial (Z_k)_{x_0}} = -2 \sum_{i=1}^{n} (p'_{e_i} - p'_{t_i}) \left(\frac{\partial p'_{t_i}}{\partial (Z_k)_{x_0}} \right) \left(\frac{p'_{e_1}}{p'_{e_i}} \right)^2 = 0 \qquad k=1,2,3 \tag{17}$$

from which it follows that

$$\sum_{i=1}^{n} (p'_{e_i}) \left(\frac{p'_{e_1}}{p'_{e_i}} \right)^2 \left(\frac{\partial p'_{t_i}}{\partial (Z_k)_{x_0}} \right) = \sum_{i=1}^{n} (p'_{t_i}) \left(\frac{p'_{e_1}}{p'_{e_i}} \right)^2 \left(\frac{\partial p'_{t_i}}{\partial (Z_k)_{x_0}} \right) \qquad k=1,2,3 \tag{18}$$

Utilizing Eq. (10) and the definition $(z_2)_{x_i} = (p'_t)_{x_i}$; that is,

$$(Z_2)_{x_i} = (T_{2,1})_{x_i} (Z_1)_{x_0} + (T_{2,2})_{x_i} (Z_2)_{x_0} + (T_{2,3})_{x_i} (Z_3)_{x_0} \tag{19}$$

it follows from differentiation that

$$\frac{\partial (Z_2)_{x_i}}{\partial (Z_1)_{x_0}} = (T_{2,1})_{x_i}; \quad \frac{\partial (Z_2)_{x_i}}{\partial (Z_2)_{x_0}} = (T_{2,2})_{x_i}; \quad \frac{\partial (Z_2)_{x_i}}{\partial (Z_3)_{x_0}} = (T_{2,3})_{x_i} \tag{20}$$

substituting Eqs. (19) and (20) into Eq. (18) yields

$$\sum_{i=1}^{n} (p'_{e_i}) (T_{2,k})_{x_i} \left(\frac{p'_{e_1}}{p'_{e_i}} \right)^2 = \sum_{i=1}^{n} \left[(T_{2,1})_{x_i} (Z_1)_{x_0} + (T_{2,2})_{x_i} (Z_2)_{x_0} + (T_{2,3})_{x_i} (Z_3)_{x_0} \right] \left[(T_{2,k})_{x_i} \left(\frac{p'_{e_1}}{p'_{e_i}} \right)^2 \right] \qquad k=1,2,3 \tag{21}$$

Equation (21) is a set of three linear algebraic equations for the three unknowns $(Z_1)_{x_0}$, $(Z_2)_{x_0}$, and $(Z_3)_{x_0}$ that correspond to u', p', and ρ' at $x=0$, respectively. Solution of these equations for a specific set of parameters G and C yields a unique set of initial conditions u', p', and ρ' at the burning propellant surface (i.e., $x=0$) that minimizes the error function E.

Determination of the Propellant Admittance

The following procedure has been utilized in the determination of the unknown propellant admittance from the measured acoustic pressure data.

1) Initially, arbitrary values of G and C are assumed. Next, $[A]_x$ is evaluated. Equation (13) is then integrated forward utilizing a fourth-order Runge-Kutta method to evaluate $[T]_x$.

2) Utilizing the calculated $[T]_x$ and the set of acoustic pressure measurements p'_{ei}, the values of u', p', and ρ' are evaluated at the propellant surface by utilizing Eq. (21).

3) $[Z]_x$ is calculated, utilizing Eq. (10).

4) E is calculated, utilizing Eq. (15).

5) This calculated error function E represents its minimum for a given set of the parameters C, G that appear in the matrix $[A]_x$. To minimize the error function E with respect to G and C, Muller's iteration technique has been utilized. This technique provides a rapid method for alternately iterating on the parameters G and C until the minimum of E, for which $(\partial E/\partial G) = (\partial E/\partial C) = 0$, is reached. The quantity $\{Z\}_{x_0}$ is calculated at every one of these iteration steps. The admittance and the response function of the burning solid propellant, the gas phase acoustic energy losses, and the axial distribution of the acoustic velocity, density, and entropy are evaluated for the minimizing set of $\{Z\}_{x_0}$, G and C.

Improved Data Acquisition Procedure

The following efforts have been made to improve the accuracy of the measured data: 1) increasing the accuracy and the dynamic range of the measured acoustic data and 2) increasing the number of pressure transducers utilized in the determination of the acoustic wave structure in the impedance tube. A combination of fifteen piezoelectric and condenser type pressure transducers were utilized. To acquire the pressure amplitude and phase data measured by the ten piezoelectric pressure transducers, a minicomputer data acquisition system is utilized. This system consists of a Hewlett Packard 2100S minicomputer with an HP 7901 disk system and a Preston GMAD-1 analog-to-digital convertor. By passing the signals measured by the pressure transducers through high pass filters, the dc component is filtered out and the ac component is amplified to levels below the A to D input voltage limitation. The software utilized for data acquisition via this system has been rewritten to include direct memory access, resulting in an increase of the maximum transfer rate to the minicomputer from 40,000 to 600,000 words/s. This dramatic increase in the data sampling rate resulted in considerably improved resolution of the measured data and a significant decrease in the experimental errors. As an example that should demonstrate the significance of the improvement, consider the following case: during a test conducted at a frequency of 600 Hz, each channel is now capable of transferring 100 samples per cycle to the minicomputer, compared to 7 samples (or words) per cycle previously.

In this connection it should be pointed out that the data presented as a single record point is an average of several thousand samples. For example, at the frequency of 600 Hz, each data point for any pressure transducer represents the averaging of 4000 samples that were measured over 40 cycles.

In addition, theoretical studies of the characteristic of the standing wave structure have indicated that the accuracy of the measured admittance depends upon the ability to accurately measure the difference between the maxima and minima of the standing wave amplitudes. To acquire such a capability, the transducer calibration procedure has been modified. Transducers located near the pressure minima are calibrated to cover the range 110-155 dB while transducers located near pressure maxima are calibrated to cover the 120-165 dB range, as shown in Fig. 2. This procedure results in a measurement system capable of measuring a 110-165 dB range that is needed to obtain the desired experimental accuracy.

Previous analytical studies had indicated that reliable determination of the admittance of a burning solid propellant requires the determination of the standing wave structure through a distance covering at least two standing wave minima. This is illustrated in Fig. 3 which describes a hypothetical, theoretically predicted, standing wave in an impedance tube for a given admittance value and different

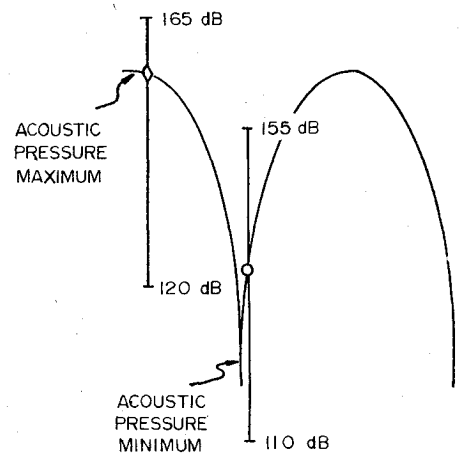

Fig. 2 Calibration ranges for pressure transducers.

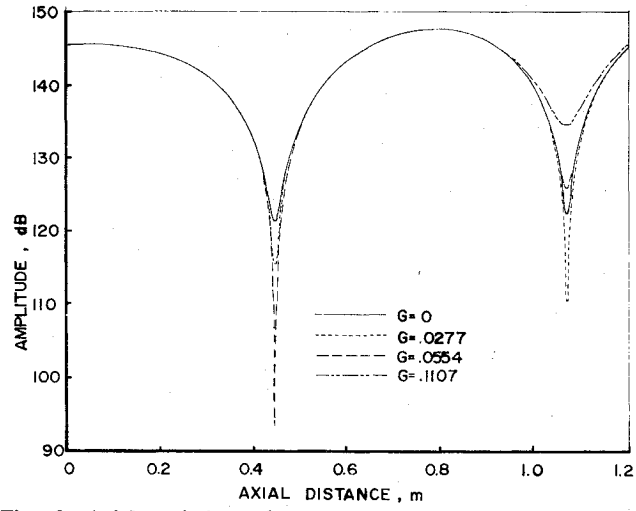

Fig. 3 Axial variation of pressure amplitude with no flow, frequency = 500 Hz, chamber pressure = 2.07 MPa, $Y_R = 0.050$, $Y_I = 0.150$.

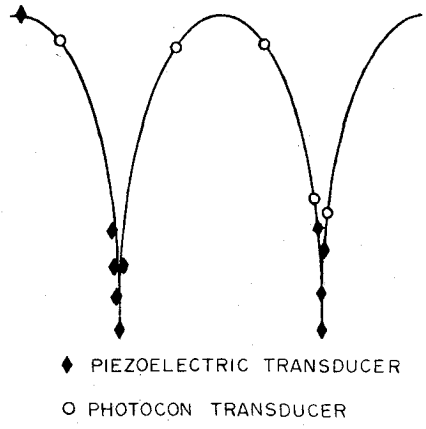

Fig. 4 Typical axial distribution of pressure transducers.

values of the gas phase loss parameter G that is representative of the acoustic energy losses in the gas phase. Figure 3 shows that pressure amplitudes corresponding to two different values of G coincides along a distance measured from the propellant sample (i.e., $x = 0$) through the first pressure minimum, but they "separate out" as the second minimum point is approached. This clearly indicates that for an accurate measurement of the bulk loss parameter G, and hence the admittance of the tested solid propellant, the standing

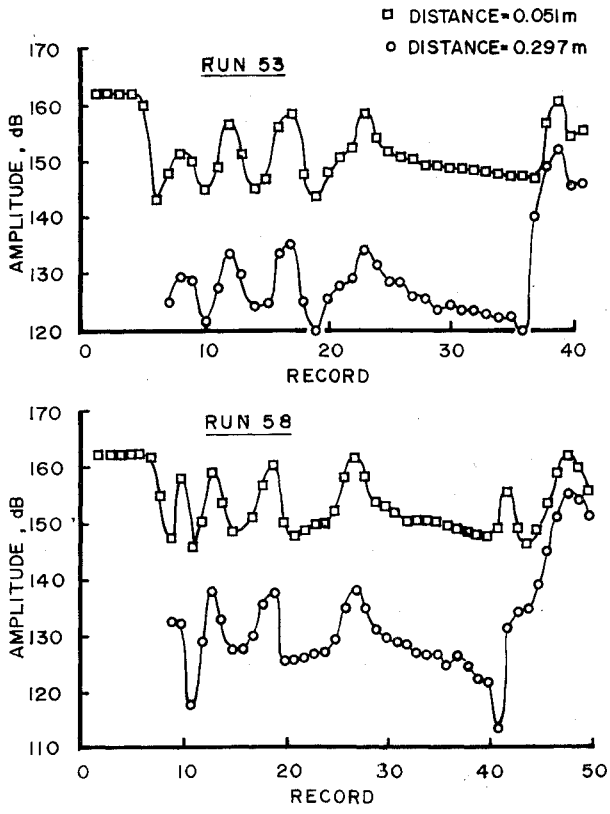

Fig. 5 Repeat runs. Propellant A-13, frequency = 675 Hz, chamber pressure = 2.07 MPa. Run 53: $Y_R = 0.012$, $Y_I = -0.157$, $G = 0.236$. Run 58: $Y_R = 0.012$, $Y_I = -0.156$, $G = 0.267$.

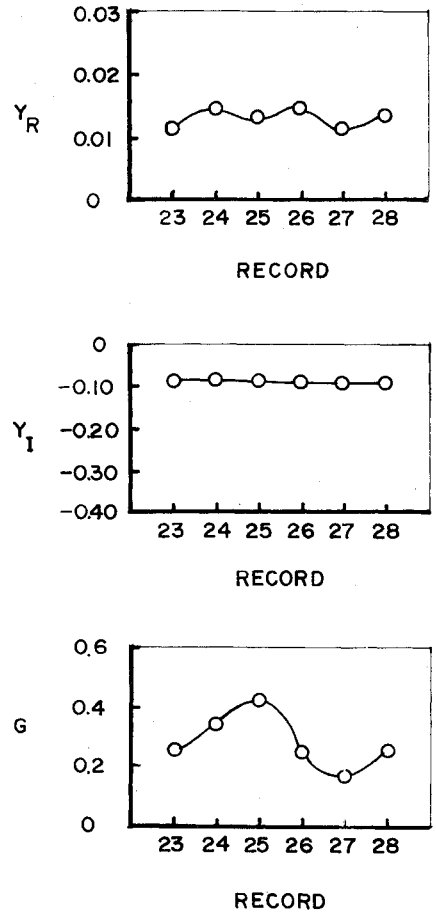

Fig. 6 Typical data measured during a given run; propellant A-14, frequency = 675 Hz, chamber pressure = 2.07 MPa.

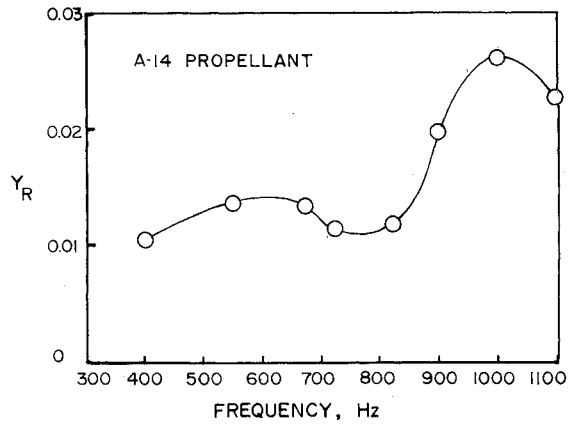

Fig. 7 Real part of admittance vs frequency; propellant A-14, chamber pressure = 2.07 MPa.

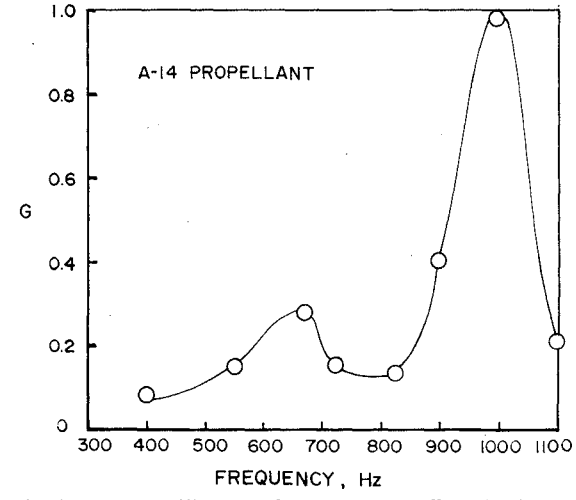

Fig. 8 Bulk loss coefficient vs frequency; propellant A-14, chamber pressure = 2.07 MPa.

wave structure has to be measured through a distance covering at least two standing wave pressure minima. To accomplish this, the number of pressure transducers has been increased from ten to fifteen. A typical distribution of the pressure transducers along the tube is shown in Fig. 4. It is worth noting that the more accurate piezoelectric pressure transducers are located near pressure minima where the greatest experimental accuracy is required.

Typical Results

Considering the complexity of the propellant admittance measurement technique, the repeatability of the experimental data was of much concern. The repeatability achieved is demonstrated in Fig. 5 showing the time evolution of the pressure amplitudes measured at distances of 0.051 and 0.297 m from the propellant surface in two different tests conducted with an A-13 propellant. Examination of this figure indicates remarkable similarity in the time evolution of the amplitudes and excellent agreement between the computed values of Y and G.

Typical admittance and gas phase loss data obtained during tests conducted with the A-14 composite solid propellant at 2.07 MPa chamber pressure are presented in Figs. 6-8 where the abscissa "record" corresponds to time. Figure 6 shows the time variation of the real and imaginary parts of the admittance Y and the bulk gas phase loss coefficient G during a test conducted with an A-14 propellant at the frequency of 675 Hz. It is noted that the real part of the admittance Y_R varies little with time while energy losses in the gas phase vary

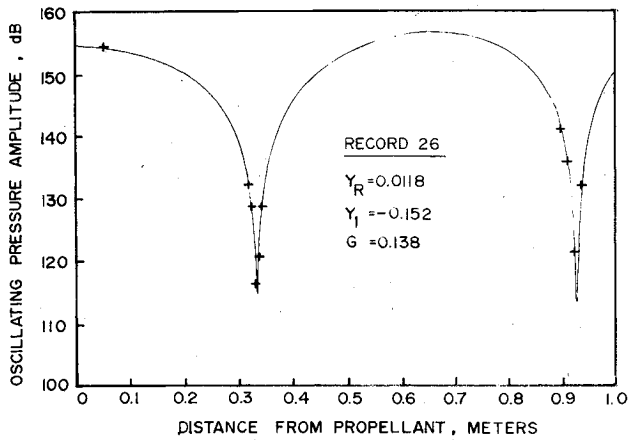

Fig. 9 Axial variation of pressure amplitude; a comparison between experimental and theoretically calculated values; record 26: propellant A-14, frequency = 625 Hz, chamber pressure = 2.07 MPa.

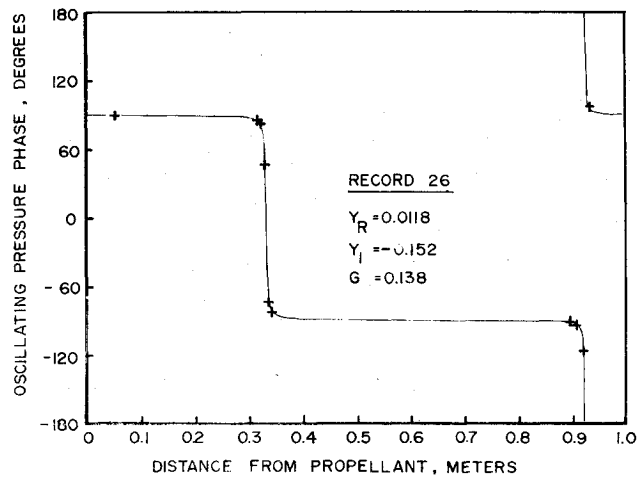

Fig. 10 Axial variation of pressure phase; a comparison between experimental and theoretically calculated values; record 26: propellant A-14, frequency = 625 Hz, chamber pressure = 2.07 MPa.

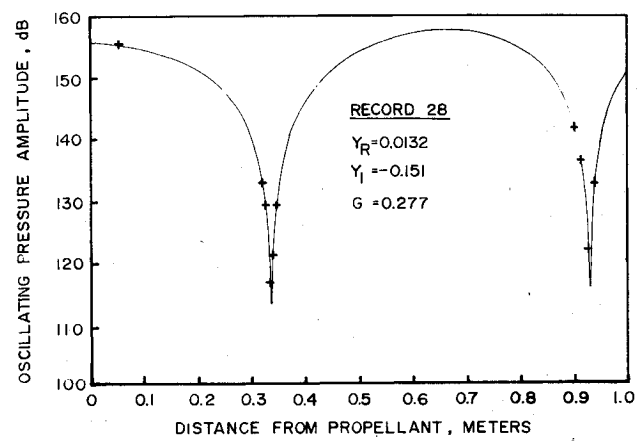

Fig. 11 Axial variation of pressure amplitude; a comparison between experimental and theoretically calculated values; record 28: propellant A-14, frequency = 625 Hz, chamber pressure = 2.07 MPa.

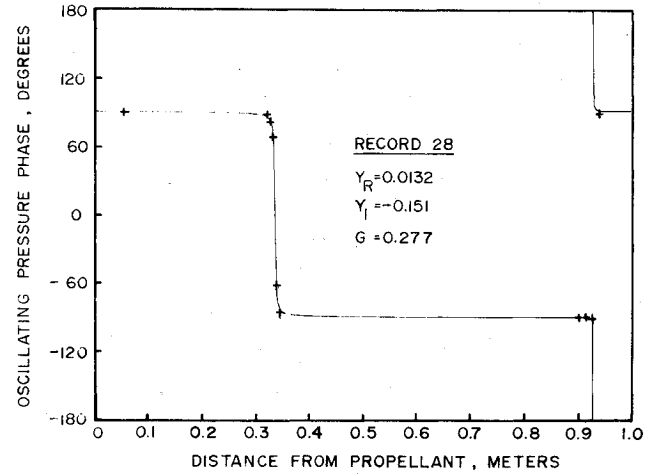

Fig. 12 Axial variation of pressure phase; a comparison between experimental and theoretically calculated values; record 28: propellant A-14, frequency = 625 Hz, chamber pressure = 2.07 MPa.

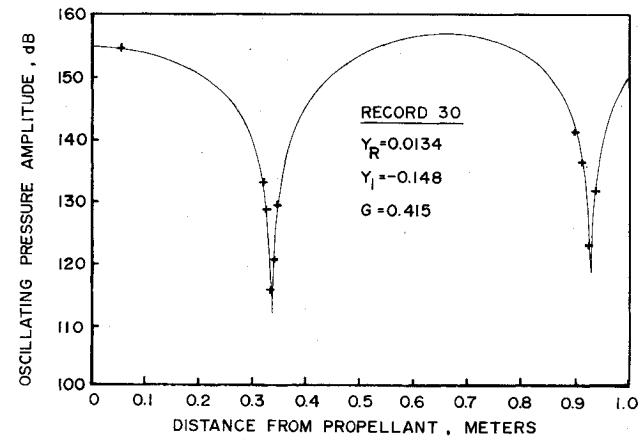

Fig. 13 Axial variation of pressure amplitude; a comparison between experimental and theoretically calculated values; record 30: propellant A-14, frequency = 625 Hz, chamber pressure = 2.07 MPa.

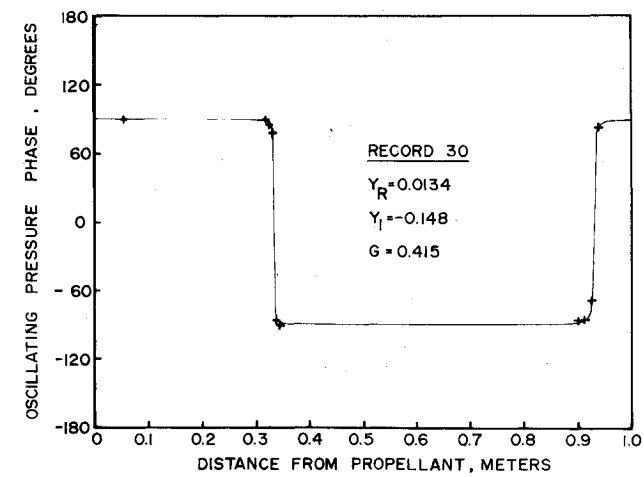

Fig. 14 Axial variation of pressure phase; a comparison between experimental and theoretically calculated values; record 30: propellant A-14, frequency = 625 Hz, chamber pressure = 2.07 MPa.

significantly with time. These figures demonstrate the ability of the impedance tube technique to measure simultaneously the time variation of acoustic energy gains and losses inside the tube during a test. Figures 7 and 8 describe the frequency dependence of the real part of the admittance Y_R and the bulk gas phase loss parameter G obtained from experiments conducted with an A-14 propellant. The Y_R curve indicates that this quantity peaks at around 1000 Hz.

Figures 9-14 provide comparisons between the predicted (based upon the determined values of the propellant admittance and the parameters G and C) impedance tube wave structure (i.e., amplitude and phase) and the measured

acoustic pressure data at three different instances during a test conducted with an A-14 propellant at the frequency of 625 Hz and chamber pressure 2.07 MPa.

These figures demonstrate the dependence of the impedance wave structure upon the gas phase losses, which are described by the parameter G that increases in magnitude from 0.138 to 0.415 during the test period covered by these figures. The effect of the change in G becomes particularly apparent when one examines Figs. 12 and 14 that show the manner in which the slope of the phase-space curve changes near the second minima point as the value of G increased from 0.277 to 0.415 between two instants of time. Yet, while the values of G change with time the calculated values for the real part of the admittance Y_R remain virtually the same, indicating an almost constant addition of acoustic energy to the gas phase by the burning propellant. Finally, it is important to note the excellent agreement shown in Figs. 9-14 between the calculated wave structure (based upon the determined values of the propellant admittance, G and C) and the measured experimental; agreement that provides further support to the applicability of the developed experimental technique.

Conclusions

Significant improvements have been achieved in the data acquisition and data reduction procedures in the solid propellant impedance tube experiment, as demonstrated by the results provided in this paper. It has been shown that the real part of the burning propellant admittance Y_R remains constant during the steady-state burn period while gas phase losses may vary significantly during the same time period. Reproducibility of the measured quantities has been established as well as the capability of this experimental technique to measure gas phase losses in the impedance tube simultaneously with the measurement of the burning solid propellant surface admittance. Finally, it has been shown that the determined propellant admittance and gas phase losses result in impedance tube wave structures that are in excellent agreement with the measured acoustic pressure data.

Appendix

$$A_{11}=\frac{1}{\bar{\rho}(\bar{c}^2-\bar{u}^2)}\left[\bar{\rho}\bar{u}\frac{d\bar{u}}{dx}-\frac{d\bar{p}}{dx}+i\omega\bar{\rho}\bar{u}+G\bar{u}\right]$$

$$A_{12}=\frac{1}{\bar{\rho}(\bar{c}^2-\bar{u}^2)}\left[\frac{\bar{u}\bar{c}^2}{\bar{p}}\frac{d\bar{\rho}}{dx}-i\omega\right]$$

$$A_{13}=-\frac{1}{\bar{\rho}}\frac{(d\bar{u})}{(dx)}-\frac{1}{\bar{\rho}(\bar{c}^2-\bar{u}^2)}\left(\frac{\bar{u}\bar{c}^2}{\bar{\rho}}\frac{d\bar{\rho}}{dx}\right)$$

$$A_{21}=-i\omega\bar{\rho}-\bar{\rho}\frac{d\bar{u}}{dx}+G-\bar{u}\frac{\bar{\rho}\bar{u}(d\bar{u}/dx)-(d\bar{p}/dx)+i\omega\bar{\rho}\bar{u}-G\bar{u}}{\bar{c}^2-\bar{u}^2}$$

$$A_{22}=-\frac{\bar{u}}{\bar{c}^2-\bar{u}^2}\left[\frac{\bar{u}\bar{c}^2}{\bar{p}}\frac{d\bar{\rho}}{dx}-i\omega\right]$$

$$A_{23}=\frac{\bar{u}}{\bar{c}^2-\bar{u}^2}\left(\frac{\bar{c}^2\bar{u}}{\bar{\rho}}\frac{d\bar{\rho}}{dx}\right)$$

$$A_{31}=-\frac{1}{\bar{u}}\left[\frac{d\bar{\rho}}{dx}+\frac{\bar{\rho}\bar{u}(d\bar{u}/dx)-(d\bar{p}/dx)+i\omega\bar{\rho}\bar{u}+G\bar{u}}{\bar{c}^2-\bar{u}^2}\right]$$

$$A_{32}=-\frac{1}{\bar{u}(\bar{c}^2-\bar{u}^2)}\left[\frac{\bar{u}\bar{c}^2}{\bar{p}}\frac{d\bar{\rho}}{dx}-i\omega\right]$$

$$A_{33}=-\frac{1}{\bar{u}}\left[-i\omega+\frac{\bar{u}\bar{c}^2(d\bar{\rho}/dx)}{\bar{\rho}(\bar{c}^2-\bar{u}^2)}\right]$$

Acknowledgment

This research was supported under AFOSR Grant 73-2571.

References

[1] "T-Burner Manual," Committee on Standardization of Combustion Instability Measurement in the T-Burner, ICRPG Working Group on Solid Propellant Combustion, Chemical Propulsion Information Agency Pub. 191, 1969.

[2] Derr, R. L., "Development and Evaluation of the Variable-Area T-Burner," AFRPL-TR-72-97, Lockheed Propulsion Co., Redland, Calif.

[3] Oberg, C. L., Ryan, N. W., and Baer, A. D., "A Pulsed T-Burner Technique," *AIAA Journal*, Vol. 6, May 1968, pp. 920-921.

[4] Brown, R. S., Erickson, J. E., and Babcock, W. R., "Combustion Instability Study of Solid Propellants," AFRPL-TR-73-42, June 1973.

[5] Strand, L. D., Magiwala, K. R., and McNamara, R. P., "Microwave Measurement of Solid Propellant Pressure-Coupled Response Function," AIAA Paper 79-1211, presented at the AIAA/SAE 15th Joint Propulsion Conference, Las Vegas, Nev., June 1979.

[6] Zinn, B. T., Salikuddin, M., Daniel, B. R., and Bell, W. A., "Solid Propellant Admittance Measurement by the Driven Tube Method," AFOSR-TR-73-2571, Aug. 1975.

[7] Salikuddin, M. and Zinn, B. T., "Adaptation of the Impedance Tube Technique for the Measurement of Combustion Process Admittances," AIAA Paper 79-0167, New Orleans, La., Jan. 1979.

[8] Perry, E. H., "Investigation of the T-Burner and It's Role in Combustion Instability Studies," Ph.D. Thesis, Daniel and Florence Guggenheim Jet Propulsion Center, California Institute of Technology, Pasadena, Calif., May 1970.

[9] Rubin, S., "Review of Mechanical Impedance and Transmission Matrix Concept," *Journal of the Acoustical Society of America*, Vol. 4, May 1967.

[10] Baum, J. D., "Experimental Determination of the Admittances of Solid Propellants by the Impedance Tube Method," Ph.D. Thesis, School of Aerospace Engineering, Georgia Institute of Technology, Atlanta, Ga., June 1980.